Available online at www.sciencedirect.com
SCIENCE DIRECT
Lithos 76 (2004) 475–490
LITHOS
www.elsevier.com/locate/lithos

Petrology of the Renard igneous bodies: host rocks for diamond in the northern Otish Mountains region, Quebec

T.C. Birkett[a,*], T.E. McCandless[b], C.T. Hood[b]

[a] *SOQUEM INC., 1000 route de Eglise, Sainte-Foy, Quebec, Canada G1V 3V9*
[b] *Ashton Mining of Canada Inc., Unit 123-930 West 1st Street, North Vancouver, BC, Canada V7P 3N4*

Received 21 June 2003; accepted 4 January 2004
Available online 10 June 2004

Abstract

The Renard igneous bodies were discovered in late 2001 as part of a regional diamond exploration program launched by Ashton Mining of Canada and SOQUEM. Nine bodies have been discovered within a 2-km-diameter area, and are comprised of root zone to lower diatreme facies rocks including kimberlitic breccia, olivine macrocrystic hypabyssal material, and brecciated country rock with minor amounts of kimberlitic material. Many mineralogical and petrographic features are common to both kimberlite and melnoite, and strict assignment of the rocks as kimberlite is not possible with these criteria alone. Whole rock trace element compositions suggest a closer affinity to Group I kimberlite, with derivation from a garnet-bearing mantle. Exceptions to conventional classification of the rocks along petrographic or mineralogical lines may be due in part to assimilation of felsic country rock into the Renard magmas at the time of emplacement. The Renard magmas were emplaced into northeastern Laurentia at 630 Ma, when the supercontinent was undergoing a change from convergent margin magmatism to rifting, the latter being associated ultimately with the opening of the Iapetus ocean.

Keywords: Kimberlite; Melnoite; Otish Mountains; Diamond; Ultramafic lamprophyre

1. Introduction

The Superior Craton hosts a wide variety of mantle-derived igneous rocks, including kimberlite (Kong et al., 1999; Girard, 2001), rocks grouped under the acronym melnoite (e.g. alnoite, aillikite; Digonnet, 1997; Digonnet et al., 2000; melilitite, Dimroth, 1970) and ultramafic lamprophyre (colloquially termed ‘wawaite’; Lefebvre et al., 2003). The Ashton–SOQUEM joint venture entered into the Quebec portion of the Superior Craton in 1996, after desktop and field studies concluded that the area was prospective for diamonds. A collection of 1700 widely spaced samples of Quaternary deposits covering 425,000 km^2 defined several anomalies, based on small counts of mantle indicator minerals present in the anomalous samples. Follow-up sampling in subsequent years resulted in the establishment of property positions by 2000. A dispersion pattern was also recognized, which contained an abundant and diverse indicator mineral assemblage, including pyrope with

* Corresponding author. Fax: +1-418-658-5459.
E-mail address: tyson.birkett@soquem.qc.ca (T.C. Birkett).

0024-4937/$ - see front matter © 2004 Elsevier B.V. All rights reserved.
doi:10.1016/j.lithos.2004.03.054

subcalcic compositions suggesting co-genesis with diamond (Gurney, 1984). The morphology of the indicators also suggested a proximal source, and follow-up samples were collected in the immediate vicinity. In mid-2001, a cobble-sized rock with surface characteristics of weathered ultramafic mantle-derived rock was discovered on surface during follow-up prospecting. Macroscopically, large anhedral

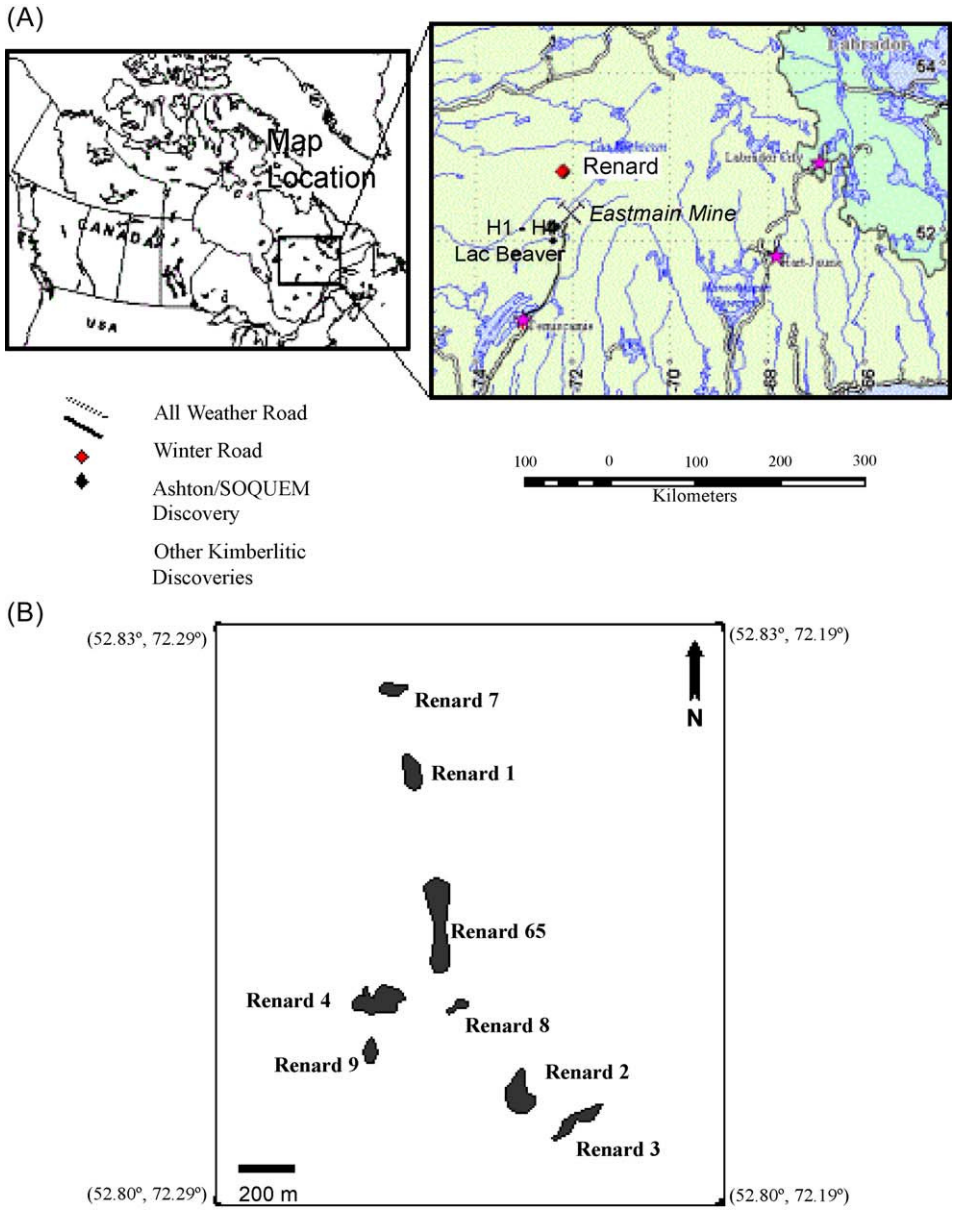

Fig. 1. (A) Location map for the Renard igneous bodies. (B) Plan view of the Renard group, with each body outline approximated from geophysical and limited drilling data.

grains of serpentine (iddingsite) after olivine were present. In thin section, the cobble revealed an unaltered internal region with anhedral forsterite in a groundmass of serpentine, phlogopite, spinel and perovskite, establishing an ultramafic igneous origin. Airborne and ground magnetic surveys were immediately conducted in the region up-ice from the cobble sample, and four geophysical anomalies were targeted for drilling, of which two were confirmed as rocks of similar composition to the cobble sample. In late 2001, the Ashton–SOQUEM joint venture announced the discovery of the Renard 1 and Renard 2 kimberlitic bodies on the Foxtrot Property in the northern Otish Mountains of Quebec, as illustrated in Fig. 1A. ('Renard' means Fox in French.) As of mid-2003, eight bodies have been discovered, with Renard 65 formed by two geophysical anomalies conjoined through recent drilling (Fig. 1B; Table 1).

Petrographic assessment of the igneous bodies began soon after their discovery, and it was recognized that the Renard bodies do not possess a coherent set of mineralogical and textural traits that would classify them as kimberlites. Both in-house and external studies established that some of the Renard bodies were more akin to rocks of melnoitic character (terminology after Scott Smith, 1995; Mitchell, 1997), and petrographically are in the overlap region between kimberlite and melnoite. Shortly thereafter, highly encouraging microdiamond results for Renard 1 and Renard 2 confirmed their diamondiferous nature, and economic assessment proceeded without concern for an unequivocal rock name assignment. The Ashton–SOQUEM venture used the term 'kimberlitic' to describe the Renard bodies in order to discuss the discoveries without implying formal name assignment for these igneous host rocks for diamond. This study represents a preliminary attempt to assign the Renard igneous bodies a formal igneous name and facies classification under scientific constraints, and to describe some basic features of their petrogenesis.

2. Regional geologic setting

The Renard bodies were emplaced through Archean metamorphic rocks of the eastern Superior Province. At present, only large-scale bedrock geological mapping is publicly available (Hocq, 1985), and prior to 2001, the nearest confirmed kimberlite was at Lac Beaver, roughly 100 km to the south of the Renard group (Girard, 2001; Fig. 1A).

Basement gneiss near the Renard bodies is believed to have been metamorphosed at upper amphibolite to lower granulite facies conditions in late Archean time. Regionally, both orthogneiss and paragneiss are present. Mafic–ultramafic and minor felsic volcanic and intrusive rocks with associated metamorphosed sedimentary rocks form the late Archean Wahamen greenstone belt, roughly 30 km south of the bodies. This supracrustal sequence was metamorphosed at a lower grade (i.e. upper greenschist facies) than nearby basement gneiss. Diabase dykes of the Mistassini swarm (2.5 Ga) intrude both of these rock types. Nearly 100

Table 1
Approximate dimensions of the Renard igneous bodies, inferred from geophysics and limited drilling, and results of preliminary testing for commercial-size diamond content

Kimberlitic body	Approximate size (m)	Sample weight tested (tonnes)	Total diamond recovered (+0.85 mm, carats)	Largest diamond recovered (carats)	Estimated diamond content (cpht)
Renard 1	150 × 100	8.80	0.78	0.12	9
Renard 2	120 × 65	4.94	3.31	0.38	67
Renard 3	145 × 25	4.88	6.54	0.73	134
Renard 4	180 × 70	8.22	4.07	0.26	50
Renard 65	300 × 60	18.44	10.0	~ 4.0[a]	54
Renard 7	150 × 60	–	–	–	–
Renard 8	75 × 40	–	–	–	–
Renard 9	160 × 40	–	–	–	–

All bodies are confirmed as diamond-bearing through microdiamond testing.
(–) Data either not yet collected or not yet processed.
[a] A four-carat diamond in drill core was detected and has not been removed from the core.

km south of the Renard bodies, resting on a profound angular unconformity, are unmetamorphosed rocks of the Otish Supergroup. These strata are dominated by conglomerate, arkose and quartzite with minor amounts of carbonate rocks preserved near the stratigraphic summit (Theriault and Bilodeau, 2002). The Otish sedimentary rocks were intruded by voluminous gabbro dykes and sills in early or middle Proterozoic time (Fahrig and Chown, 1973). Rare fragments of siltstone and carbonate rocks in the Renard bodies suggest that Paleoproterozoic cover rocks, Otish or approximately equivalent Sakami formation, were present at the time of emplacement.

A radiometric age for the Renard igneous bodies has been obtained through U–Pb age determination of groundmass perovskite, analysed at the University of Alberta under contract with Geospec Consultants. The model age, based on a weighted average of $^{206}Pb/^{238}U$ ratios from multiple fractions is 631.6 ± 3.5 Ma (2σ) for hypabyssal material from the Renard 1 body. This age is similar to that reported for the Wemindji kimberlites (629 ± 29 Ma; Letendre et al., 2003) but older than the Lac Beaver kimberlite (551 ± 3 Ma; Girard, 2001; Moorhead et al., 2002). Other significant events in and around Quebec near this time included emplacement of the giant Sept-Îles layered gabbro complex 565 ± 4 Ma (Higgins and van Breeman, 1998), aillikite dykes in the Torngat Mountains (544 ± 12 Ma; Digonnet et al., 2000), the St-Honoré carbonatite (629–656 Ma; Vallée and Dubuc, 1970), propagation of the Saint Lawrence rift system and correlated alkalic volcanism (544 ± 4 Ma; Kumarapeli et al., 1989) and intrusion of the Grenville dykes (590_{-1}^{+2} Ma; Kamo et al., 1995). Collectively, these events are broadly correlative with the conversion from subduction magmatism to rifting in northern Laurentia (750–600 Ma, Keppie et al., 2003).

3. Geology of the Renard igneous bodies

3.1. Form

The Renard bodies exhibit irregular-to-elongate forms (Fig. 1B), although at present this interpretation is based entirely on geophysical data and limited drill hole information, as none of the bodies crops out at surface. Renard bodies range in size from 0.3 to 1.5 ha in area. In cross-section, the bodies are steep-sided breccia pipes partially surrounded by irregular breccia zones in peripheral country rock. Two textural varieties of kimberlitic rock are present: olivine macrocrystic material and kimberlitic breccia. Every igneous body is covered by 6–20 m of glacial material, and contacts are in most cases approximated from ground geophysics. Contacts with enclosing country rock can vary from sharp to transitional, with no apparent correlation with geophysical signature. Sharp contacts seem to be more prevalent when the country rock exhibits strong gneissic fabric, or an absence of fabric altogether such as in some high-grade amphibolite rocks. Delineation of the Renard bodies is still in its early stages and early interpretations may be resolved or modified as further data become available.

3.2. Facies division

The bulk of each body is comprised of kimberlitic breccia surrounded by minor, peripheral zones of variably brecciated country rock. The latest event in each body is emplacement of macrocrystic xenolith-free material as dykes and/or sills of apparent widths ranging from a few centimeters to several meters that cross-cut tuffisitic breccia, brecciated country rock, and non-brecciated basement rock adjacent to the bodies.

Kimberlitic breccias are formed by 15–90 vol.% of locally derived heterolithic xenoliths in a kimberlitic matrix, including common olivine macrocrysts and their serpentinsed pseudomorphs. They have little or no calcite as determined by a lack of reaction to dilute HCl. Pelletal lapilli with kernels of macrocrystic olivine or xenoliths of crustal rock are present throughout diatreme facies units, though rarely more abundant than a few percent. For this reason, it is appropriate to describe the Renard breccias as tuffisitic kimberlite breccias without implying a formal facies assignment.

Macrocrystic material is the less abundant kimberlitic rock, and is distinguished by common-to-abundant disseminated calcite as determined by reaction to dilute HCl. Country rock xenoliths are rare, but olivine macrocrysts are ubiquitous with some reaching several cm in longest dimension. Uniform-textured groundmass is the norm in these rocks, although segregationary-textured groundmass is lo-

cally present in larger bodies; in facies terminology (e.g. Scott Smith, 1996) this rock would be considered hypabyssal.

Country rock breccias peripheral to some bodies are composed of gneiss and tonalite host rocks, which consist principally of gneisses of intermediate composition with the common mineral assemblage plagioclase, biotite, orthopyroxene and quartz. Country rock breccias also have significantly disturbed zones of tonalite gneiss and medium- to coarse-grained non-deformed granite dykes that intrude the gneissic rocks. Collectively these units comprise the country rock xenolith suite in the breccias, in amounts ranging from 15% to 90% of the total rock volume, and in some cases are without a detectable kimberlitic component. Grain size reduction in some zones has produced rocks with the appearance of an arkose at the macroscopic scale.

3.3. Petrographic characteristics

In thin section, hypabyssal facies rocks have a relatively simple mineralogy and texture, and visually appear to be the least-contaminated by country rock. Macrocrysts of subhedral-to-anhedral olivine are dispersed in a groundmass of ilmenite, spinel, perovskite, Ti-magnetite-ulvöspinel, phlogopite and apatite in a mesostasis dominated by calcite (Fig. 2A,B). Partially-to-completely serpentinised second-generation olivine is also observed, as is non-altered monticellite. Atoll-textured spinels are present but only locally abundant (Fig. 2C,D). Necklace texture is present, though rare and of limited development. Plates of phlogopite–kinoshitalite series mica poikilitically enclose groundmass unaltered monticellite, perovskite, apatite, and iron oxides.

Breccias have a more complex mineralogy, with olivine macrocrysts, commonly serpentinised, and in some examples, rimmed by groundmass diopside in a mesostasis of phlogopite and serpentine. The earliest groundmass is medium-to-dark brown, weakly magnetic, with a small amount of calcite present. This groundmass is locally replaced, commonly with obliteration of textures such as lapilli, by a medium-to-pale green groundmass, slightly more granular in appearance, non-magnetic, with no detectable calcite. The groundmass recrystallisation may be due to low-temperature processes, possibly post emplacement.

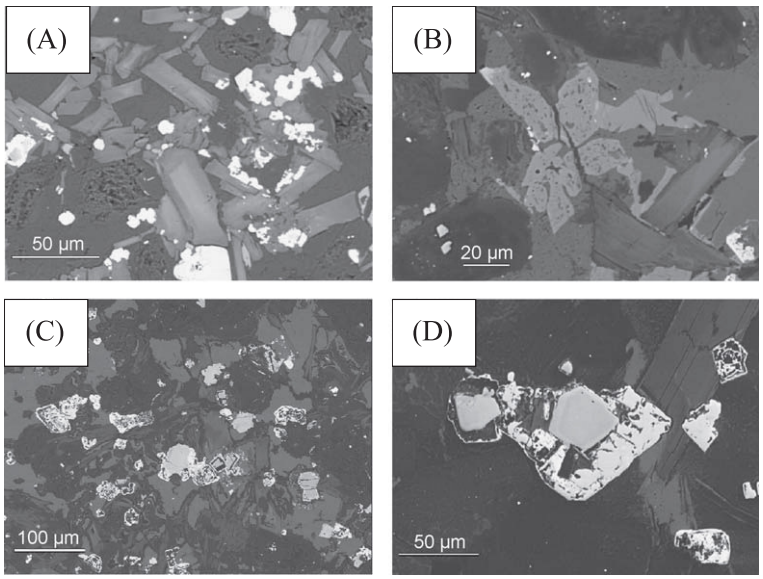

Fig. 2. Backscattered scanning electron images from hypabyssal facies samples of Renard bodies. (A) Zoned groundmass phlogopite laths with iron oxides in a mesostasis of carbonate and serpentine. (B) Radiating splays of apatite with phlogopite laths and iron oxides in a groundmass of carbonate. (C) Atoll spinels and phlogopite in a mesostasis of carbonate. (D) Closer view of the atoll spinels, showing a nucleus of Cr-rich spinel with differing composition indicated by lower brightness.

Table 2
Representative olivine, orthopyroxene and monticellite compositions from the Renard igneous bodies

	Olivine					Orthopyroxene		Montice llite		
	1	2	3	4	5	1	2	1	2	3
SiO_2	41.22	41.21	41.69	41.16	41.00	57.72	57.80	36.85	37.81	37.75
TiO_2	0.01	0.00	0.00	0.00	0.03	0.09	0.12	0.04	0.00	0.00
Al_2O_3	0.02	0.03	0.04	0.01	0.03	0.82	0.86	0.02	0.03	0.01
Cr_2O_3	0.07	0.04	0.09	0.12	0.02	0.50	0.17	0.03	0.00	0.00
Fe_2O_3						0.85	1.05			
MgO	50.24	51.46	52.15	50.68	49.38	34.69	34.88	21.57	23.33	23.36
CaO	0.05	0.01	0.01	0.04	0.07	1.16	1.13	33.33	34.88	34.85
MnO	0.13	0.09	0.04	0.13	0.15	0.13	0.08	0.19	0.25	0.24
FeO	8.77	7.46	6.28	8.08	9.56	4.66	4.40	7.82	4.03	4.41
NiO	0.39	0.36	0.35	0.41	0.38	0.11	0.13	0.09	0.10	0.03
BaO	0.06	0.04	0.02	0.03	0.00	0.00	0.00	0.00	0.00	0.00
Na_2O	0.02	0.02	0.02	0.01	0.01	0.19	0.22	0.04	0.00	0.04
Total	100.97	100.72	100.70	100.67	100.62	100.92	100.84	99.95	100.43	100.69
Mg#	0.91	0.93	0.94	0.92	0.90	0.90	0.92	0.83	0.91	0.90

Both macroscopic and thin section examination reveal extensive physical and chemical interaction between Renard magmas and adjacent host rocks. Most rock fragments are subangular-to-subrounded, but a population of well-rounded rock fragments is also observed. In many areas, visual evidence of crustal xenolith and host magma interaction can be observed. Broken mineral grains are common and feldspar cleavage fragments are significant groundmass components, which when reacted commonly show concentric reaction bands. Rock fragments observed in thin section are converted to assemblages of carbonate, serpentine, sericite and chlorite. Mafic minerals in the crustal xenoliths have typically strongly reacted with the magma; of these, garnet reacts most and biotite least. Liberated subhedral crystals of biotite are commonly dispersed in breccia groundmass to the extent that they are indistinguishable from phlogopite at hand sample scale. In thin section, these grains display identical pleochroism with those of xenoliths of crustal derivation and are interpreted as locally derived xenocrysts. Efficient disaggregation and assimilation of country rock units into the Renard magmas may have contributed to difficulties in

Table 3
Representative compositions of phlogopite from the Renard igneous bodies

	1	1	2	2	3	3	3	4	4	5	5	6	6	7	7
	Core	Rim	Core	Rim	Rim	Mid	Core	Core	Rim	Core	Rim	Core	Rim	Core	Rim
SiO_2	35.20	36.17	36.17	37.30	39.83	32.10	31.64	37.86	32.96	35.16	35.72	41.08	41.06	35.84	41.72
TiO_2	2.35	1.46	3.28	1.96	0.56	1.04	1.12	0.56	2.49	1.77	0.58	0.27	0.07	3.45	1.55
Al_2O_3	15.92	18.37	14.63	15.15	14.69	18.33	18.26	17.77	18.04	16.80	17.44	13.19	0.74	15.82	10.99
Cr_2O_3	0.01	0.02	0.09	0.10	0.04	0.06	0.00	0.00	0.03	0.00	0.00	0.19	0.06	0.05	0.02
MgO	21.80	23.39	11.62	20.79	26.47	22.83	22.89	25.03	21.63	22.42	25.24	27.65	26.55	21.18	24.62
CaO	0.04	0.02	0.03	0.10	0.05	0.02	0.01	0.06	0.07	0.09	0.19	0.06	0.03	0.08	0.03
MnO	0.09	0.03	0.14	0.20	0.01	0.03	0.03	0.07	0.08	0.06	0.07	0.02	0.28	0.11	0.06
FeO	7.06	4.31	21.04	10.30	2.74	3.42	3.36	3.30	5.61	6.00	4.55	3.00	15.99	6.98	6.26
NiO	0.01	0.03	0.06	0.04	0.03	0.09	0.10	0.07	0.00	0.00	0.03	0.01	0.03	0.06	0.04
BaO	2.96	1.81	0.00	0.00	0.03	10.51	10.61	1.61	5.81	3.13	1.99	0.27	0.00	2.51	0.00
Na_2O	0.04	0.03	0.37	0.06	0.02	0.15	0.04	0.04	0.06	0.09	0.05	0.09	0.14	0.05	0.08
K_2O	9.09	9.81	9.57	9.37	10.75	6.93	6.87	10.19	8.40	9.13	8.90	10.35	10.13	9.14	10.02
Total	94.56	95.44	96.99	95.37	95.23	95.51	94.91	96.55	95.17	94.65	94.78	96.17	95.07	95.26	95.38

assigning these rocks to a strictly kimberlite or melnoite classification.

4. Mineralogy and mineral composition

Analyses of minerals by electron microprobe were obtained at Laval University, Quebec on the Cameca, SX100, and performed by Marc Choquette, Eng. Natural and synthetic standards were used in the analytical routines; data were reduced using the PAP system of Pouchou and Pichoir (1985). Typical silicate and oxide mineral analyses were obtained with operating conditions of 15.0 kV acceleration and 20.0 nA beam current.

4.1. Olivine, orthopyroxene and monticellite

Magnesian olivine is an abundant component of all Renard kimberlites. Macrocrysts and their serpentinised pseudomorphs are ubiquitous. Serpentine after groundmass olivine is common to all facies. Macrocrysts are typically 2 cm or less in length and rounded, although a few up to 4 cm have been noted. A few mantle-derived xenoliths of olivine with orthopyroxene, clinopyroxene or garnet have been observed. Olivine analyses are limited to macrocryst cores because of serpentinisation, and range from Fo_{88} to Fo_{93} with few outliers (Table 2). CaO is low, n.d. to 0.1 wt.%; Cr_2O_3 is also low (<0.1 wt.%). Concentrations of MnO are near 0.1 wt.%, and NiO ranges from 0.3 to 0.4 wt.%. Orthopyroxene has also been detected in some samples, though it is typically partially-to-completely serpentinized and indistinguishable from olivine. Mg numbers of 0.90–0.92 suggest that orthopyroxene is derived from disaggregated peridotite (Table 2). As a groundmass phase, monticellite is present as small subhedral crystals in some hypabyssal facies samples. The grains are characterized by NiO contents less than 0.1 wt.%, and relatively high MnO of 0.2–0.3 wt.% (Table 2).

4.2. Phlogopite

Phlogopite from hypabyssal facies samples shows variation in composition from Ba-phlogopite–kinoshitalite to tetraferriphlogopite (Table 3). There are several phlogopite compositions that warrant further consideration as they plot within, and away from, compositional trends attributed to igneous rocks related to kimberlite (Fig. 3A). Samples from the least-contaminated rocks display iron-rich cores with development of iron-poor mantles, followed in a few cases by red tetraferriphlogopite rims rich in iron but depleted in Al and Ti. This pattern of initial iron depletion is typical of kimberlite but distinct from other potassic ultramafic rocks. Aluminium in phlog-

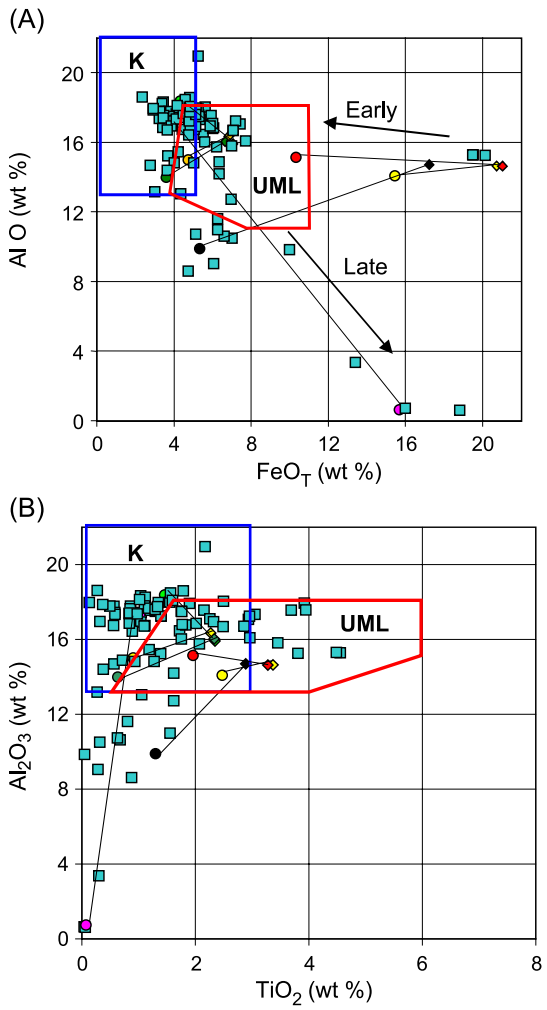

Fig. 3. (A) Groundmass phlogopite compositions in FeO_T–Al_2O_3 space, with boxes for kimberlite (K) and ultramafic lamprophyre (UML) from Mitchell (1997) and Mitchell et al. (1999). Diamonds and circles indicate analyses of cores and rims of individual crystals, single analyses are squares. (B) Phlogopite compositions in TiO_2–Al_2O_3 space.

opite commonly increases slightly during crystallisation, but in some cases decreases slightly (Fig. 3B).

4.3. Iron-titanium oxides

A variety of oxide minerals that differ from kimberlitic FeTi oxides in composition and/or texture are present in the Renard bodies. Isolated spinel crystals and cores of atoll-textured grains are aluminous magnesio-chromite, probably micro-xenocrysts. Typical compositions have 8–10 wt.% Al_2O_3, 13–15 wt.% MgO, and 52–56 wt.% Cr_2O_3 (Table 4). Contents of TiO_2 are low at 1–5%, and MnO is generally not detected. Crystals show limited chemical zonation, with only moderate continuous zoning toward the margins of chromite cores (Fig. 4). Later-crystallising spinels are Ti-poor magnesioferrite–magnetite which typically form wide mantles on chromite cores. Spinel evolutionary trends fall in trend T2 of Mitchell (1986) on a 'reduced iron' diagram of $Fe_T^{2+}/(Fe_T^{2+}+Mg)$ versus Ti/(Ti + Al + Cr) (Fig. 4A). This trend is considered atypical for kimberlite. In Cr/(Cr + Al) and Ti/(Ti + Al + Cr) space, the evolutionary trend leaves typical kimberlite space giving a pattern approaching that of ultramafic lamprophyres (Fig. 4B). These analyses are similar to those reported for a variety of ultramafic lamprophyres by Mitchell et al. (1999).

Rare groundmass ilmenite forms two populations: small euhedra with planar faces and small, spongy grains of corroded aspect. It is a high MnO (13–22 wt.%) type with high Fe_2O_3 and low Ti and Mg (Table 5). These ilmenites differ from the highly magnesian ilmenite typical of kimberlite. The spongy grains are believed to be residual to a late-magmatic reaction, and may be relics after euhedral ilmenite or perovskite. Recalculation commonly yields 40–50 mol% $MnTiO_3$, 60–50 mol% $FeTiO_3$ and negligible $MgTiO_3$. Ilmenite with high Mn is known in some kimberlites but seems relatively rare (e.g. Beard et al., 2000).

Perovskite is a common groundmass mineral, occurring as small subhedral-to-subrounded dark brown crystals. With respect to some elements, it is typical of kimberlite (and orangeite) with moderate ThO_2 (n.d at <0.1–1 wt.%), Nb_2O_5 (0.6–1.9 wt.%), REE (3.4–6.1 wt.% La_2O_3 to Sm_2O_3) and Na_2O (0.2–0.5 wt.%). In terms of strontium, most grains have contents near 0.2 wt.%, although analyses from two samples show unusually high SrO near 1 wt.% (Table 6). The higher SrO contents are atypical for perovskite from unevolved kimberlite (Mitchell, 1995b, p. 221) and melnoite.

4.4. Apatite

Apatite forms radiating splays of groundmass crystals associated with serpentine and calcite. Locally crystals have hollow cores, interpreted as reflecting rapid skeletal growth. Rare cases of small skeletal grains with abundant extremely fine-grained inclusions have been noted (Fig. 2B). Compositionally, apatite generally shows low total REE contents, with total of light rare earth oxides typically less than 1.0 wt.% for La_2O_3 to Sm_2O_3. A few grains show higher contents, up to 2 wt.%. Strontium contents cover a wider range, from 0.1 to 8 wt.% SrO, although the majority contains less than 1 wt.%. The latter compositional feature is at odds with groundmass apatite

Table 4
Representative spinel compositions from the Renard igneous bodies

	1	2	3	4	5	5	5	6	6	7	7	7	8	9	10	11
					Core	Rim 1	Rim 2	Core	Rim	Core	Rim 1	Rim 2				
TiO_2	1.98	2.34	3.34	3.74	1.53	1.10	3.23	1.41	1.21	1.26	1.80	3.50	4.87	2.10	5.14	4.00
Al_2O_3	10.53	8.68	9.45	9.30	12.26	11.56	3.53	14.46	10.65	15.50	12.98	3.43	7.58	4.21	8.03	6.40
Cr_2O_3	54.71	56.97	53.63	52.50	55.62	56.66	1.54	52.09	56.39	51.20	48.67	1.80	0.53	0.29	0.15	0.11
Fe_2O_3	8.26	8.14	9.09	10.18	5.75	5.44	67.42	5.67	6.16	6.02	10.43	66.48	56.59	65.01	58.45	62.00
Nb_2O_5	0.05	0.00	0.00	0.00	0.00	0.02	0.00	0.03	0.00	0.01	0.00	0.01	0.03	0.03	0.01	0.01
MgO	14.78	14.32	13.80	13.99	16.19	16.23	14.66	14.90	14.17	15.84	15.20	14.34	9.78	10.14	10.08	9.49
MnO	0.00	0.00	0.00	0.00	0.00	0.00	0.53	0.00	0.00	0.00	0.00	0.50	0.72	1.01	0.57	0.73
FeO	11.54	12.12	12.97	12.63	9.30	8.89	8.30	11.38	12.21	10.09	10.50	8.59	15.06	14.21	15.74	16.53
ZnO	0.01	0.12	0.03	0.08	0.06	0.05	0.03	0.08	0.00	0.10	0.06	0.10	0.03	0.01	0.05	0.08
Total	101.85	102.69	102.32	102.42	100.70	99.95	99.25	100.00	100.79	100.02	99.62	98.76	95.18	96.98	98.22	99.35

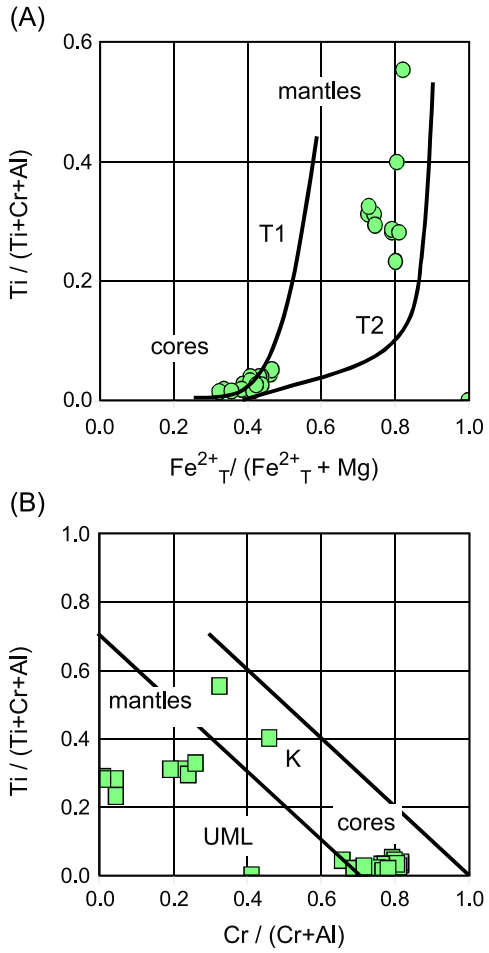

Fig. 4. Cation ratios of spinels projected in the spinel prism after Mitchell (1997). (A) Analyses follow the trend 2 (T2) pattern atypical for kimberlites, but (B) with affinities to ultramafic lamprophyres.

in kimberlite and melnoite, both of which have low Sr. Silica is commonly present at 0.8 to 3 wt.% SiO_2. A linear relationship between rare earths and strontium (Table 7) reflects the chemical environment of crystallization with these trace elements concentrated in residual magma.

4.5. Carbonate minerals

Calcite is the dominant carbonate mineral in all specimens studied to date. Small amounts of magnesite have been recognized in one sample of hypabyssal facies material. Calcite is present as anhedral masses with serpentine and as rare tabular crystals. All compositions analysed are low in Sr, with no Sr peak observed on inspection of EDS spectra.

4.6. Secondary garnet

Small amounts of garnet have been observed in one sample as elongate masses in the cleavage of otherwise unaltered phlogopite. Compositionally approaching andradite, these grains have less than 0.03 wt.% ZrO_2 and less than 0.02 wt.% Cr_2O_3. Similar textures have been reported for hydrogrossular–hydroandradite within biotite from low-grade altered granitoids (Freiberger et al., 2001), where a retrograde origin on cooling has been suggested.

4.7. Xenocryst minerals and diamond content

The Renard bodies were discovered after indicator minerals with favourable mineral composition were discovered in till samples. Xenocryst minerals recovered from Renard drill samples consist of ilmenite, chromian spinel, forsterite, aluminous enstatite, chromian clinopyroxene, and chromian pyrope. Though not the subject of this study, the xenocryst mineral suite exhibits compositional trends that are supportive of derivation from mantle in which diamond is stable. Noteworthy is the rare occurrence of forsterite megacrysts exceeding 8 cm in length, with clusters of included pyrope, the latter having a subcalcic composition supporting the presence of diamond in the mantle parent rock.

All of the Renard bodies are diamond-bearing, with diamond contents up to 134 cpht (carats per hundred

Table 5
Representative groundmass ilmenite compositions from the Renard igneous bodies

	1	2	3	4	5
TiO_2	35.02	42.80	52.03	49.94	48.59
Al_2O_3	0.19	0.13	0.05	0.01	0.00
Cr_2O_3	0.08	0.01	0.04	0.13	0.12
Fe_2O_3	32.26	15.05	0.00	0.89	3.30
Nb_2O_5	0.05	0.00	0.82	1.14	1.14
MgO	2.86	1.31	0.11	0.02	0.07
MnO	13.27	16.34	3.79	20.57	21.84
FeO	13.12	19.70	32.44	24.12	21.51
ZnO	0.07	0.06	0.00	0.02	0.00
Total	96.91	95.40	89.17	96.69	96.44

Table 6
Representative compositions of groundmass perovskite from the Renard igneous bodies

	1	2	3	4	5	6	7	8	9
TiO_2	54.08	53.52	53.38	53.75	53.58	52.64	51.94	53.19	52.93
ThO_2	1.00	0.41	0.24	0.72	0.31	0.39	0.69	0.17	0.10
Al_2O_3	0.52	0.53	0.53	0.70	0.51	0.67	0.64	0.55	0.70
Cr_2O_3	0.04	0.00	0.00	0.04	0.00	0.02	0.00	0.04	0.00
Nb_2O_5	1.10	1.78	1.93	0.94	1.92	1.13	1.57	1.59	1.35
La_2O_3	1.25	1.20	1.25	1.25	1.46	1.12	1.30	1.33	1.12
Ce_2O_3	3.09	2.31	2.57	2.78	2.55	2.71	3.27	2.96	2.24
Pr_2O_3	0.36	0.26	0.35	0.25	0.23	0.37	0.41	0.37	0.11
Nd_2O_3	1.19	0.86	0.82	1.02	0.80	1.02	1.04	0.99	0.83
Sm_2O_3	0.21	0.11	0.08	0.14	0.12	0.00	0.17	0.22	0.12
MgO	0.05	0.04	0.03	0.04	0.02	0.04	0.06	0.08	0.00
CaO	35.58	36.10	35.94	36.32	36.19	36.43	35.34	36.75	38.06
MnO	0.02	0.00	0.07	0.00	0.00	0.03	0.00	0.00	0.00
FeO	1.84	2.45	2.40	2.39	2.18	2.41	2.33	2.21	2.38
ZnO	0.00	0.00	0.19	0.04	0.00	0.00	0.00	0.11	0.00
SrO	0.22	0.88	0.95	0.31	0.96	0.26	0.25	0.32	0.35
Na_2O	0.51	0.42	0.39	0.32	0.37	0.31	0.45	0.30	0.16
Total	101.04	100.86	101.12	101.02	101.18	99.50	99.26	100.99	100.28

tones), though estimations are presently based on small samples (less than 10 tonnes per body) and are insufficient to represent actual grades (Table 1).

5. Whole rock composition

Whole rock analyses were obtained on split core samples by XRF for major elements, Leco for CO_2, and ICP-MS for trace elements, all at ALS Chemex, Vancouver.

The extensive contamination of the Renard bodies with country rock has been visually established, from the macro to the microscale, and whole rock analysis of any of the kimberlitic breccias would be pointless. From a visual perspective, the hypabyssal phase of the Renard bodies is the least-contaminated, and selected hypabyssal portions from Renard 1, 2, 3, 4, 5 and 7 were analysed for major and trace elements (Table 8). All but three analyses have SiO_2 and Al_2O_3 contents less than 35 and 5 wt.%, respectively (Fig. 5A), which are the maximum values proposed by Mitchell (1986),

Table 7
Representative compositions of groundmass apatite from the Renard igneous bodies

	1	2	3	4	5	6	7	8	9	10
P_2O_5	40.20	42.98	41.36	41.49	38.97	38.00	38.21	37.61	39.89	40.97
SiO_2	1.04	0.13	0.97	0.84	0.52	0.81	1.43	1.67	1.00	0.75
La_2O_3	0.03	0.03	0.09	0.12	0.39	0.55	0.01	0.08	0.09	0.16
Ce_2O_3	0.02	0.05	0.09	0.01	0.48	0.88	0.02	0.31	0.14	0.25
Pr_2O_3	0.00	0.00	0.02	0.05	0.27	0.11	0.00	0.04	0.10	0.10
Nd_2O_3	0.11	0.14	0.04	0.05	0.17	0.44	0.03	0.23	0.01	0.00
Sm_2O_3	0.00	0.07	0.00	0.00	0.04	0.00	0.03	0.13	0.00	0.02
CaO	54.66	55.00	53.50	54.35	50.35	46.54	54.54	53.79	54.67	54.77
FeO	0.28	0.17	0.11	0.00	0.12	0.19	0.19	0.23	0.21	0.21
SrO	0.32	0.10	2.14	1.12	4.43	7.64	0.63	0.57	0.25	0.87
BaO	0.00	0.00	0.11	0.13	0.05	0.00	0.05	0.00	0.09	0.09
Na_2O	0.25	0.05	0.06	0.07	0.04	0.05	0.15	0.17	0.31	0.08
Total	96.91	98.72	98.48	98.22	95.83	95.21	95.28	94.83	96.76	98.27

Table 8
Whole rock compositions for hypabyssal material from the Renard igneous bodies (R = Renard)

Location	R1	R1	R2	R2	R3	R3	R4	R4	R4	R5	R7
SiO_2	33.40	33.98	42.25	31.40	38.17	33.97	33.74	35.09	31.35	28.60	36.94
TiO_2	0.49	0.59	0.89	0.85	0.99	0.63	1.81	0.99	0.96	0.90	0.82
Al_2O_3	1.61	1.63	5.17	1.41	2.12	1.81	2.03	2.10	1.66	2.49	2.68
Fe_2O_3	8.56	7.47	6.49	8.21	5.74	8.27	9.12	7.65	6.25	7.74	8.63
MnO	0.15	0.12	0.12	0.10	0.15	0.17	0.13	0.08	0.14	0.12	0.13
MgO	35.50	32.20	22.34	30.40	33.34	31.33	34.40	31.32	28.75	26.52	32.62
CaO	5.91	6.27	7.57	8.03	2.80	5.26	4.49	4.98	10.10	12.16	2.04
Na_2O	0.05	0.02	0.37	<0.01	0.01	0.02	0.03	0.05	0.01	0.04	0.10
K_2O	0.97	1.52	2.92	0.52	0.86	0.70	0.72	0.83	0.52	0.42	1.00
P_2O_5	0.44	0.21	0.42	0.24	0.26	0.31	0.31	0.60	0.13	0.62	0.34
LOI	11.00	13.90	9.68	16.85	13.35	15.40	10.90	14.15	18.15	18.50	12.60
CO_2	2.6	4.3	3.2	6.2	1.7	3.8	2.7	3.1	7.9	9.1	1.3
Ag	<1	<1	<1	<1	<1	<1	<1	<1	<1	<1	<1
Ba	1545	688	1325	1400	1345	1460	902	1830	429	853	1110
Co	94.8	85.6	70.6	88.6	97.2	88.1	91.1	89.5	89	71.2	89.1
Cr	2060	2010	1440	2000	2260	1900	2200	2000	1760	1480	2220
Cs	0.8	1	1.9	0.5	0.7	0.8	0.5	0.7	0.7	1	1.4
Cu	41	37	<5	34	56	49	18	77	<5	33	38
Ga	4	4	9	4	6	5	5	11	4	5	5
Hf	1	1	3	1	2	2	1	2	1	2	1
Mo	<2	<2	<2	<2	<2	<2	<2	<2	<2	<2	<2
Nb	89	88	138	164	152	246	178	223	120	200	152
Ni	1605	1470	1030	1535	1355	1470	1350	1470	1660	1065	1595
Pb	5	<5	5	5	5	8	6	7	6	8	5
Rb	76.1	99.3	154.5	45.7	56.6	63	44.5	64	54.2	43.3	75.9
Sn	1	1	1	1	1	1	1	1	1	1	1
Sr	740	447	538	546	502	397	264	198.5	727	813	338
Ta	5.5	6.6	7.8	11.2	11.2	12.7	12.9	13.3	7.3	12.8	9.4
Th	10	11	17	17	6	19	18	21	12	15	15
Tl	<1	<1	<1	<1	<1	<1	<1	<1	<1	1	<1
U	1.4	1.2	2.5	2	1.3	2.8	1.7	2.3	2.4	4	2.3
V	63	58	80	52	124	40	35	21	75	82	57
W	<1	<1	<1	<1	5	1	1	1	<1	1	1
Y	6.1	5.6	8.5	4.2	4.8	7.7	6.7	6.9	6.2	9.3	6.3
Zn	57	49	38	52	58	44	19	41	38	25	40
Zr	37.5	32.7	89.1	48	71.6	89.2	35.9	73	31	71.3	53.7
La	61.4	78.2	106.5	104	67.7	135.5	123.5	123.5	96.8	162	62.7
Ce	104.5	130.5	173	192	112.5	242	216	256	163	278	113.5
Pr	10.8	13.4	17.7	19.8	11.8	24.7	21.8	27.3	16.4	27.6	12.2
Nd	35.1	43.3	58.4	65.4	39.2	81.9	71.7	90.4	54.5	89.1	41.6
Sm	4.6	5.4	7.7	7.8	4.9	10.6	8.3	10.9	7	10.8	5.4
Eu	1.2	1.4	1.8	1.8	1.2	2.6	1.9	2.4	1.7	3	1.3
Gd	4.1	4.9	6.9	6.7	4.1	8.9	7.3	9.1	6	9.8	4.7
Tb	0.4	0.5	0.7	0.6	0.4	0.8	0.7	0.7	0.5	0.9	0.5
Dy	1.4	1.5	2.3	1.5	1.2	2.4	2	2.1	1.7	2.6	1.6
Ho	0.2	0.2	0.3	0.2	0.2	0.3	0.3	0.3	0.2	0.4	0.2
Er	0.7	0.6	1	0.6	0.5	1	0.8	0.9	0.8	1.1	0.8
Tm	<0.5	<0.5	<0.5	<0.5	<0.5	<0.5	<0.5	<0.5	<0.5	<0.5	<0.5
Yb	0.4	0.4	0.6	0.2	0.3	0.5	0.4	0.3	0.4	0.5	0.4
Lu	0.1	0.1	0.1	<0.1	<0.1	0.1	0.1	<0.1	0.1	0.1	0.1

Major oxides are in weight percent, trace elements are in parts per million.

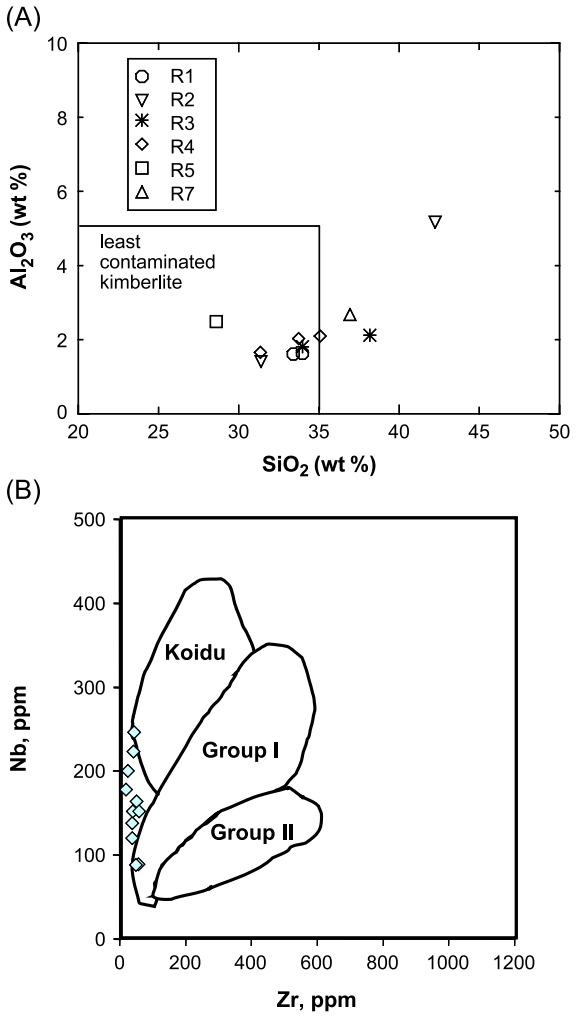

Fig. 5. (A) SiO_2–Al_2O_3 of hypabyssal intrusive rocks from the Renard bodies. The majority plot within the region thought to be uncontaminated by crustal material (after Mitchell, 1986). (B) Zr–Nb comparison to Group I kimberlites and related igneous rocks (fields after Taylor et al., 1994).

to indicate kimberlite that is uncontaminated by crustal material. Although these values may not be applicable to melnoite, they are extended to hypabyssal facies samples of the Renard igneous bodies which are chemically close to kimberlite and suggest that at least all but three samples represent relatively uncontaminated material.

Major element compositions of Renard samples broadly overlap Group I kimberlites in most elements, although P_2O_5 is relatively low.

With respect to trace element compositions, the Renard bodies have considerably lower Hf and Zr than is observed for most Group I kimberlites, with a range of values nearly identical to kimberlites from the Karelian region of eastern Finland (O'Brien and Tyni, 1999; Fig. 5B), although Nb concentrations overlap various types of kimberlite.

With the caveat that reported kimberlite compositions cover a wide range (Mitchell, 1995b), the Renard samples show relatively low Pb and Cs, a significantly smaller than usual negative K anomaly, a marked negative Sr anomaly, and modest negative anomalies of Hf and Zr (Fig. 6A). Kimberlites commonly show much larger negative K and Sr anoma-

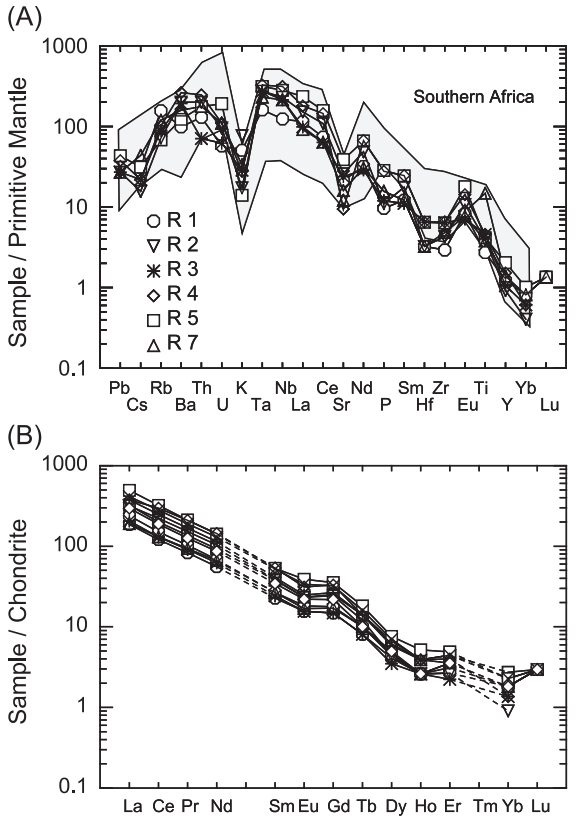

Fig. 6. Trace element plots for selected Renard (R) bodies. (A) Incompatible element distribution diagram normalized to primitive mantle comparing Group I kimberlites (shaded area; data from Smith et al., 1985) with Renard samples; (B) chondrite-normalized rare earth spectra of Renard samples (normalizing values from Sun and McDonough, 1989).

lies, although with wide variation in data from various occurrences. Melnoites, in contrast to kimberlites, commonly show smaller negative anomalies of K and Sr. Chondrite-normalised rare earth distribution patterns for the Renard bodies show a steep slope from La to Lu, no Eu-anomalies and are thus unexceptional except for a slightly elevated content of middle REE (Fig. 6B). Much of the difference among samples of Fig. 6 can be attributed to varying dilution of the groundmass by macrocrystic olivine. Thus the various samples show extensive overlap. Ratios of Nb to Ti and Zr are unusually high for kimberlitic rocks, although Zr/Hf (30–50) and Nb/Ta (10–20) are typical for mantle-derived magmas. Concentrations of light REE are higher than normal for kimberlites. The overall incompatible element signatures are similar to average Group I kimberlites (Smith et al., 1985), with the exceptions noted above. Comparison with melnoites is limited by availability of published analyses. In general, melnoites show higher profiles from Ce to Lu in Fig. 6B than Renard samples or kimberlites.

6. Discussion

6.1. Nomenclature

Rocks which cannot be reliably classified as kimberlite, lamproite or melilitite in the past were commonly placed in the melnoite 'category'. The earlier history of the term melnoite has been reviewed by Scott Smith (1995). Originally an acronym for melilite and alnoite, melnoite has become a stem name with genetic implications which presently groups rocks of the lamprophyric facies of the melilitite clan (Mitchell, 1994a,b, 1996, 1997). We follow the usage of Mitchell, and furthermore use the term 'kimberlitic' to describe rocks such as the Renard bodies which fall in many respects within the definition of kimberlite but would be excluded on the basis of certain inconsistencies, as discussed below.

6.2. Classification of the Renard bodies

While hypabyssal facies samples of the Renard igneous bodies exhibit many features that allow classification as Group I kimberlites, elements such as Zr and Hf do not conform strictly to Group I characteristics (Figs. 5 and 6). Some of these exceptions might be due to assimilation of felsic country rock. This possibility is certainly supported from a petrographical and mineralogical perspective within the breccia facies. Macrocrystic hypabyssal facies samples, however, show only weak correlations among possible contaminants (Si, K, Al) and with the exception of one sample analyzed from Renard 2 significant crustal contamination can be excluded. Phlogopite from the Renard bodies supports rock classification as kimberlite, with many analyses falling within the specified compositional region (Fig. 3). However, phlogopite chemically zoned to aluminous biotite is also present, as is aluminous spinel, Sr-enriched apatite, and Mn-enriched ilmenite. From a classification perspective, aluminous biotite is present only in melnoite, whereas the other mineral compositions do not fit either a melnoite or kimberlite classification. With respect to the groundmass spinels, atoll texture is the common textural expression in kimberlite, and is typically absent in other related rocks. The Renard bodies locally contain minor amounts of atoll-textured spinel, which in some cases have the required Mg–Cr rich compositions. However, many spinels deviate in composition and are more aluminous than accepted for kimberlite, orangeite, melnoite or lamproite (Mitchell, 1995a, 1997). Each of these minerals could be modified from more kimberlitic compositions by chemical reaction with felsic country rocks. At present, mineral compositional responses to contamination via activities of components in kimberlitic magmas are not quantified. The limited extent of contamination, as indicated by major-element data, suggests that the mineral compositions are a primary feature of these magmatic rocks. This raises the possibility (though beyond the scope of this study), that some melnoites are classified as such due to interaction with crustal rocks, and in a purely uncontaminated state would be more akin to Group I kimberlite in terms of texture, mineralogy and chemistry. Considering trace element compositions of Renard samples, anomalously low Zr, for example, is unlikely to result from limited contamination by local country rocks.

6.3. Implications for diamond exploration

For diamond exploration, it is useful to have a general term to describe all potential igneous host rocks for diamond. Nearly all such rocks share similarities. For example, all have sampled similar parts of the mantle in their ascent. Anhedral olivine macrocrysts are a common feature, which impart a pseudoporphyritic texture. Some or all of the mantle indicator assemblage is present, such as magnesioilmenite, pyrope garnet, chrome diopside, and/or picrochromite. Recovery of microscopic diamonds from kilogram-sized samples of an igneous host rock is further support that the magma has sampled diamond-bearing mantle. As each of these criteria is met, the rock continues to share characteristics with kimberlite. With the now-current use of melnoite restricted to rocks of the melilitite clan, rocks can be described as 'kimberlitic' in an exploration program, and classified along academic guidelines at a point when such research is necessary. In the interim, it is premature to assume that a mantle-derived igneous rock with evidence of derivation from the diamond stability field should be excluded from economic assessment because it is not kimberlite sensu stricto.

Table 9
Summary of petrograhic features of the Renard igneous bodies compared to kimberlite and melnoite (characteristics and terminology after Mitchell, 1997)

	Kimberlite	Renard igneous rocks	Melnoite
Olivine (macrocrysts)	abundant	abundant	rare to abundant
Olivine (groundmass)	common	common	common
Monticellite	common	present	present
Mica (macrocrysts)	minor	not observed	present
Mica (phenocrysts)	rare	not observed	present
Mica (groundmass)			
–Phlogopite	kinoshitalite	both trends	Al-biotite
Spinel	trend 1	trend 2	trend 2
–Atoll	very common	present	? present
–Necklace	present	very rare	? present
Perovskite	Sr, REE-poor	some Sr, REE-rich	Sr, REE-poor
Apatite	Sr, REE-poor	some Sr, REE-rich	Sr, REE-poor
–Skeletal	rare	present	present
Calcite	abundant	abundant	present to abundant
Mn-ilmenite	rare	present	rare
Macrocryst suite	common	present	rare
Chemical signature	intermediate between the two		

7. Conclusions

Renard rocks share features with both kimberlite and melnoite. They should be considered intermediate members of a spectrum of magma compositions (Table 9). Whole rock major and trace element compositions of samples from hypabyssal facies intervals suggest a closer affinity to Group I kimberlite, with derivation from a garnet-bearing mantle lithosphere. Details of mineral compositions, on the other hand, suggest ties to melnoites. Exceptions to conventional classification of the rocks along petrographic or mineralogical lines may be due in part to assimilation of felsic country rock into the Renard magmas at the time of emplacement. Isotopic analyses might eventually help quantify contamination and test this hypothesis.

The Renard bodies are presently exposed at the lower diatreme or root zone level, though some likely breached the surface as indicated by the presence of rare lapilli and sedimentary xenoliths derived from the Otish Supergroup. At the time of their emplacement at 630 Ma, northeastern Gondwanaland was undergoing a change from convergent margin magmatism to rifting, the latter being ultimately associated with the opening of the Iapetus ocean.

Acknowledgements

The authors thank the Ashton–SOQUEM joint venture for support and permission to publish these early findings on the Renard igneous bodies. Critical help and comments from B. Clements, R.T. Lucas, A. O'Connor, D. Skelton, J. Ward, A. Berry, C. Mircea, L. Boyer, E. Gofton and E. O'Brien-Russell (Ashton), and from P. Bertrand and G. Poirier (SOQUEM) have advanced understanding of the Renard bodies. Critical reviews by Ingrid Kjarsgaard and Roy Eccles and

editorial comments by R.H. Mitchell greatly improved the quality of the paper and are acknowledged with appreciation.

References

Beard, A.D., Downes, H., Hegner, E., Sablukov, S.M., 2000. Geochemistry and mineralogy of kimberlites from the Arkhangelsk Region, NW Russia: evidence for transitional kimberlite magma types. Lithos 51, 47–73.

Digonnet, S., 1997. A petrogeochemical study of kimberlites from the Torngat Mountains, New Quebec (in French). Unpublished MSc thesis, University of Quebec, Montreal.

Digonnet, S., Goulet, N., Bourne, J., Stevenson, R., Archibald, D., 2000. Petrology of the Abloviak dykes, New Quebec: evidence for a Cambrian diamondiferous alkaline province in northeastern North America. Can. J. Earth Sci. 37, 517–533.

Dimroth, E., 1970. Meimechites and carbonatites of the Castignon Lake Complex, New Quebec. Neues Jahrb. Petrol. Mineral. Abh. 130, 247–274.

Fahrig, W.F., Chown, E.H., 1973. The paleomagnetism of the Otish Gabbro from north of the Grenville Front, Quebec. Can. J. Earth Sci. 10, 1556–1564.

Freiberger, R., Hecht, L., Cuney, M., Morteani, G., 2001. Secondary Ca–Al silicates in plutonic rocks: implications for their cooling history. Contrib. Mineral. Petrol. 141, 415–429.

Girard, R., 2001. Caracterisation de l'intrusion Kimberlitique du lac Beaver, Monts Otish—Petrographie et Mineralogy. Ressources Naturelles Quebec, Government Province Quebec, Canada, MB 2001-08, 23 pp.

Gurney, J.J., 1984. A correlation between garnets and diamonds in kimberlite. In: Harris, P.G., Glover, J.E. (Eds.), Kimberlite Occurrence and Origin: A Basis for Conceptual Models in Exploration. Geology Department and University Extensions, University of Western Australia, Perth, Western Australia, pp. 143–146. Special Publication 8.

Higgins, M.D., van Breeman, O., 1998. The age of the Sept Iles layered mafic intrusion, Canada: implications for the Late Neoproterozoic/Cambrian history of southeastern Canada. J. Geol. 106, 421–431.

Hocq, M., 1985. Géologie de la région des Lacs Campan et Cadieux. Ministère de l'énergie et des Ressources, Québec. ET 83-05, 178 pp.

Kamo, S.L., Krough, T.E., Kumarapeli, P.S., 1995. Age of the Grenville dyke swarm, Ontario-Quebec: implications for the timing of Iapetan rifting. Can. J. Earth Sci. 32, 273–280.

Keppie, J.D., Nance, R.D., Murphy, J.B., Dostal, J., 2003. Tethyan, Mediterranean, and Pacific analogues for the Neoproterzoic–Paleozoic birth and development of peri-Gondwanan terranes and their transfer to Laurentia and Laurussia. Tectonphysics 365, 195–219.

Kong, J.M., Boucher, D.R., Scott Smith, B.H., 1999. Exploration and Geology of the Attawapiskat Kimberlites, James Bay Lowland, Northern Ontario, Canada. In: Gurney, J.J., Gurney, J.L., Pascoe, M.D., Richardson, S.H. (Eds.), Proceedings of the 7th International Kimberlite Conference. University of Cape Town, Cape Town, pp. 452–467.

Kumarapeli, P.S., Dunning, G.R., Pinston, H., Shaver, J., 1989. Geochemistry and U–Pb zircon age of commenditic metafelsites of the Tibbit Hill Formation, Quebec Appalachians. Can. J. Earth Sci. 26, 1374–1383.

Lefebvre, N.S., Kopylova, M.G., Kivi, K.R., Barnett, R.L., 2003. Diamondiferous volcaniclastic debris flows of Wawa, Ontario, Canada. (extended abstract). Programme and Abstracts of the 8th International Kimberlite Conference (CD-ROM). 5 pp.

Letendre, J., L'Heureux, M., Nowicki, T.E., Creaser, R., 2003. The Wemindji kimberlites: exploration and geology. (Extended Abstract) Programme and Abstracts of the 8th International Kimberlite Conference (CD-ROM). 5 pp.

Mitchell, R.H., 1986. Kimberlites—Mineralogy, Geochemistry, and Petrology. Plenum, New York. 442 pp.

Mitchell, R.H., 1994a. The lamprophyric facies. Mineral. Petrol. 51, 137–146.

Mitchell, R.H., 1994b. Suggestions for revisions to the terminology of kimberlites and lamprophyres from a genetic viewpoint. In: Meyer, H.O.A., Leonardos, O.H. (Eds.), Kimberlites, Related Rcosk and Mantle Xenoliths, Proceedings of the Fifth International Kimberlite Conference. Companhia de Pesquisa de Recursos Minerais Special Publication, Rio de Janeiro, Brazil, vol. 1/A, pp. 15–26.

Mitchell, R.H., 1995a. The role of petrography, lithogeochemistry in exploration for diamondiferous rocks. In: Griffin, W.L. (Ed.), Diamond Exploration: Into the 21st Century. J. Geochem. Explor., vol. 53, pp. 339–350.

Mitchell, R.H., 1995b. Kimberlites, Orangeites and Related Rocks. Plenum, New York.

Mitchell, R.H., 1996. The melilite clan. In: Mitchell, Rh.H. (Ed.), Undersaturated Alkaline Rocks: Mineralogy, Petrogenesis and Economic Potential. Short Course Series - Mineralogical Association of Canada, vol. 24, pp. 123–151.

Mitchell, R.H., 1997. Kimberlites, Orangeites, Lamproites, Melilitites, and Minettes: A Petrographic Atlas Almaz Press, Thunder Bay, Ontario. 243 pp.

Mitchell, R.H., Scott Smith, B.H., Larsen, L.M., 1999. Mineralogy of Ultramafic Dikes from the Sarfartoq, Sisimiut and Maniitsoq Areas, West Greenland. In: Gurney, J.J., Gurney, J.L., Pascoe, M.D., Richardson, S.H. (Eds.), Proceedings of the 7th International Kimberlite Conference. University of Cape Town, Cape Town, pp. 574–583.

Moorhead, J., Giriard, R., Heaman, L., 2002. Caractérisation des Kimberlites au Québec. Ministère des Ressources naturelles du Québec, Government Province Quebec, Canada, DV 2002-10, 36 pp.

O'Brien, H.E., Tyni, M., 1999. Mineralogy and geochemistry of kimberlites and related rocks from Finland. In: Gurney, J.J., Gurney, J.L., Pascoe, M.D., Richardson, S.H. (Eds.), Proceedings of the 7th International Kimberlite Conference. University of Cape Town, Cape Town, pp. 625–636.

Pouchou, J.L., Pichoir, F., 1985. "PAP" $\varphi(\rho z)$ procedure for improved quantitative microanalysis. Microbeam Anal. 20, 104–106.

Scott Smith, B.H., 1995. Petrology and diamonds. Explor. Min. Geol. 4, 349–366.

Scott Smith, B.H., 1996. Kimberlites. In: Mitchell, Rh.H. (Ed.), Undersaturated Alkaline Rocks: Mineralogy, Petrogenesis and Economic Potential. Short Course Series - Mineralogical Association of Canada, vol. 24, pp. 217–243.

Smith, C.B., Gurney, J.J., Skinner, E.M.W., Clement, C.R., Ebrahim, N., 1985. Geochemical character of southern African kimberlites: a new approach based on isotopic constraints. Trans. Geol. Soc. S. Afr. 88, 180–267.

Sun, S.-S., McDonough, W.F., 1989. Chemical and isotopic systematics of oceanic basalts: implications for mantle composition and processes. In: Saunders, A.D., Norry, M.J. (Eds.), Magmatism in the Ocean Basins. Spec. Publ. - Geol. Soc. Lond., vol. 42, pp. 313–345.

Taylor, W.R., Tompkins, L.A., Haggerty, S.H., 1994. Comparative geochemistry of West African kimberlites: evidence for a micaceous kimberlite endmember of sublithospheric origin. Geochim. Cosmochim. Acta 58, 4017–4037.

Theriault, R., Bilodeau, C., 2002. Geological Map of Quebec. Edition 2002. Ministère des Ressources Naturelles du Québec, Government Province Quebec, Canada, DV2002-07.

Vallée, M., Dubuc, F., 1970. The St-Honoré carbonatite complex, Quebec. Trans. CIMM 73, 346–356.